

Influence of Small-Angle Intersheet Scattering on the Galvanomagnetic Properties of Polyvalent Metals: Application to Cadmium*

RICHARD A. YOUNG, J. RUVALDS, AND L. M. FALICOV

Department of Physics and the James Franck Institute, University of Chicago, Chicago, Illinois 60637

(Received 26 September 1968)

The influence of small-angle scattering between different sheets of Fermi surface on the galvanomagnetic properties of metals is calculated using an idealized Fermi surface. The effects of the small-angle scattering are included explicitly in the solution of the Boltzmann equation. The theoretical results are applied to experimental measurements of the transverse magnetoresistance and Hall resistivity of cadmium and Cd-Zn alloys with the magnetic field parallel to the [0001] direction. Excellent agreement is obtained for the observed properties of the Hall resistivity as well as the magnetoresistance. The agreement between theory and experiment indicates the inadequacy of using *only* a relaxation-time approximation in dealing with the transport properties of these metals.

I. INTRODUCTION

THE galvanomagnetic properties of metals have provided a powerful tool for the investigation of the electronic structure of solids.^{1,2} In particular, the magnetic field dependence of the transverse magnetoresistance for various directions of the applied magnetic and electric fields has yielded a wealth of information about the Fermi-surface topology. We limit the present discussion to the "semiclassical" regime, i.e., the phenomena associated with the motion of an electron which can be considered to be a quasiparticle with a general dispersion law $\epsilon(\mathbf{k})$ and which satisfies Fermi-Dirac statistics. Thus, we neglect quantum-mechanical effects, such as the de Haas-Shubnikov oscillations, which are due to the quantization of the electron orbit areas in the presence of a magnetic field.¹

Lifshitz, Azbel, and Kaganov³ have formulated a theory of the galvanomagnetic properties of metals which has been quite successful in elucidating various anomalous features in the experimental results.^{1,2,4} Their theory emphasizes the connection between the Fermi-surface geometry and the galvanomagnetic properties while ignoring the detailed nature of the scattering mechanisms. The results of their theory are summarized in Table I. In addition, Lifshitz *et al.* find that the magnetoresistance of a metal, $\rho(H)$, should satisfy Kohler's rule, i.e., that

$$\frac{\Delta\rho}{\rho(0)} = \frac{\rho(H) - \rho(0)}{\rho(0)}$$

is a function only of $|\mathbf{H}|[\rho(0)]^{-1}$.

* Work supported partially by the National Science Foundation, the U. S. Office of Naval Research, and the Advanced Research Projects Agency.

¹ For a survey of the theoretical and experimental work on galvanomagnetic properties of metals see, e.g., R. G. Chambers, in *The Fermi Surface*, edited by W. A. Harrison and M. B. Webb (John Wiley & Sons, Inc., New York, 1962), p. 100.

² E. Fawcett, *Advan. Phys.* **13**, 139 (1964), and references cited therein.

³ I. M. Lifshitz, M. Ya. Azbel', and M. I. Kaganov, *Zh. Eksperim. i Teor. Fiz.* **30**, 220 (1955); **31**, 63 (1956) [English transl.: *Soviet Phys.—JETP* **3**, 143 (1956); **4**, 41 (1957)].

⁴ I. M. Lifshitz and V. G. Peschanskii, *Zh. Eksperim. i Teor.*

Striking departures from Kohler's rule, as well as from the field dependence of the magnetoresistance discussed above (Table I), have been found experimentally in metals which exhibit magnetic-breakdown effects.^{5,6} In such cases interband transitions, i.e., electron tunneling between different sheets of the Fermi surface, can occur and thereby change the connectivity of the orbits. These effects, and their influence on the galvanomagnetic properties, have been extensively studied both theoretically and experimentally.⁶

Recent experimental results for a number of metals (e.g., potassium, cadmium, and aluminum) have shown drastic departures from the predicted field dependence of the magnetoresistance (Table I) and from Kohler's rule.⁷⁻¹⁷ The latter discrepancies, however, cannot be attributed to magnetic-breakdown effects and consequently require a detailed investigation of the effects of scattering on the behavior of the magnetoresistance. For example, in the case of potassium, localized umklapp scattering has profound effects on the mag-

Fig. 35, 1251 (1958); **38**, 188 (1960) [English transl.: *Soviet Phys.—JETP* **8**, 875 (1959); **11**, 137 (1960)].

⁵ M. H. Cohen and L. M. Falicov, *Phys. Rev. Letters* **8**, 231 (1961).

⁶ R. W. Stark and L. M. Falicov, in *Progress in Low Temperature Physics*, edited by C. J. Gorter (North-Holland Publishing Co., Amsterdam, 1967), p. 235.

⁷ A. B. Pippard, in *Proceedings of the Alta Lake Summer School on Electrons in Metals*, British Columbia, 1967 (unpublished).

⁸ F. E. Rose, Ph.D. thesis, Cornell University, 1964 (unpublished).

⁹ P. A. Penz, Ph.D. thesis, Cornell University, 1967 (unpublished).

¹⁰ A. Penz and R. Bowers, *Solid State Commun.* **5**, 341 (1967).

¹¹ D. C. Tsui and R. W. Stark, *Phys. Rev. Letters* **19**, 1317 (1967).

¹² A. N. Gerritsen and O. P. Katyal, preceding paper, *Phys. Rev.* **178**, 1037 (1969).

¹³ C. G. Grenier, K. R. Efferson, and J. M. Reynolds, *Phys. Rev.* **143**, 406 (1966).

¹⁴ V. G. Volotskaya, *Zh. Eksperim. i Teor. Fiz.* **44**, 80 (1963) [English transl.: *Soviet Physics—JETP* **17**, 56 (1963)].

¹⁵ R. J. Balcombe, *Proc. Roy. Soc. (London)* **A275**, 113 (1963).

¹⁶ E. S. Borovik, V. G. Volotskaya, and N. Ya. Fogel, *Zh. Eksperim. i Teor. Fiz.* **45**, 46 (1963) [English transl.: *Soviet Physics—JETP* **18**, 34 (1964)].

¹⁷ E. S. Borovik and V. G. Volotskaya, *Zh. Eksperim. i Teor. Fiz.* **48**, 1554 (1965) [English transl.: *Soviet Phys.—JETP* **21**, 1041 (1965)].

TABLE I. Magnetic field dependence of the galvanomagnetic properties of metals in the high-field limit.

Type of orbits and state of compensation	Transverse magnetoresistance	Transverse Hall voltage
I. All closed orbits uncompensated ($n_e \neq n_h$)	Saturates	$H/(n_e - n_h)$
II. All closed orbits compensated ($n_e = n_h$)	H^2	H
III. Open in direction perpendicular to H and making angle α with current	$H^2 \cos^2 \alpha$	H

netoresistance¹⁸ and provides an explanation for the anomalous features of the experimental results. The explicit dependence of the magnetoresistance on the electron scattering has been considered by Pippard¹⁹ and by Jones and Sondheimer.²⁰ Pippard has investigated the effect of small-angle scattering on the longitudinal magnetoresistance in copper, and Jones and Sondheimer have treated the case of weakly anisotropic scattering for cubic metals with spherical Fermi surfaces.

Young¹⁸ has investigated theoretically the influence of localized scattering between different sheets of the Fermi surface (intersheet scattering) on the galvanomagnetic properties of metals by means of the following scattering model (Fig. 1). Consider two channels, A and B , and a variable ϕ which specifies the position along the channels. On each channel a function $S(\phi_A, \phi_B) = S(\phi_B, \phi_A)$ is introduced, such that $S(\phi_A, \phi_B)d\phi_A$ is the probability per unit time that a particle at ϕ_B will be scattered into the interval between ϕ_A and $\phi_A + d\phi_A$. For convenience, $S(\phi_A, \phi_B)$ is assumed to be nonzero only in a region $0 \leq \phi_A, \phi_B \leq \Delta$ and intrachannel scattering is neglected. Starting with an incoming particle in channel A at time $t=0$, the problem is to determine the probability that the particle is in channel A at $t = \infty$.

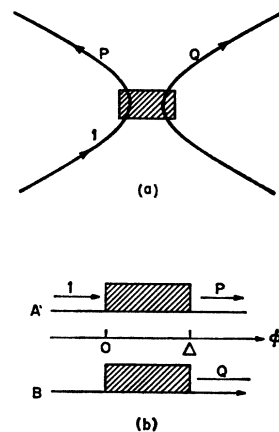


FIG. 1. Model used in computing effects of intersheet scattering: (a) two pieces of Fermi surface whose close proximity makes intersheet scattering (shaded region) likely; (b) two-channel problem used to compute P and Q as defined in part (a).

¹⁸ Richard A. Young, *Phys. Rev.* **175**, 813 (1968).

¹⁹ A. B. Pippard, *Proc. Roy. Soc. (London)* **A282**, 464 (1964); **A305**, 291 (1968).

²⁰ M. C. Jones and E. H. Sondheimer, *Phys. Rev.* **155**, 567 (1967).

The problem may be reduced to solving a set of coupled integro-differential equations with appropriate boundary conditions.¹⁸ Denoting the drift velocity in either channel by $\omega = d\phi_A/dt = d\phi_B/dt$, and assuming that $S(\phi_A, \phi_B) = C$ ($0 \leq \phi_A, \phi_B \leq \Delta$), where C is a constant, the probability P that the particle will emerge in the incident channel is given by

$$P = \frac{1}{2} \left(1 + \frac{e^{-1/\omega\mathcal{T}} - \frac{1}{2}\omega\mathcal{T}(1 - e^{-1/\omega\mathcal{T}})}{1 - \frac{1}{2}\omega\mathcal{T}(1 - e^{-1/\omega\mathcal{T}})} \right), \quad (1.1)$$

where $\mathcal{T}^{-1} = C\Delta^2$, and \mathcal{T} is the typical scattering time for the two-channel model. The probability that the particle will emerge in the opposite channel is then given by $Q = 1 - P$. When applying (1.1) to an orbit on the Fermi surface, ω is taken to be the cyclotron frequency ($\omega = eH/m^*c$) of the orbit in question. The functions P and Q are plotted as a function of $\omega\mathcal{T}$ in Fig. 2.

At this point it is worthwhile to make a comparison of the intersheet scattering process with magnetic breakdown. Although both processes involve tunneling between different sheets of the Fermi surface, the similarities end there. Magnetic breakdown in a result of interband transitions, while the intersheet scattering can take place within the same band and exhibits a completely different dependence on the magnetic field strength, i.e., the probability of switching to another channel due to scattering *decreases* with the magnetic field strength as contrasted with the magnetic breakdown tunneling probability [$p^2 = \exp(-H_0/H)$, where H_0 is a constant] which is enhanced by the field. Thus in the limit of very large magnetic fields, the particle travels very fast through the scattering region and the probability of scattering to another channel tends to zero. For low fields, on the other hand, the particle is scattered many times while it passes through the scattering region and is equally likely to emerge from either channel. The latter result is quite different from the magnetic-breakdown probability which tends to zero for very low magnetic fields.

Due to the fact that the orbit geometry and the degree of compensation can be changed by scattering

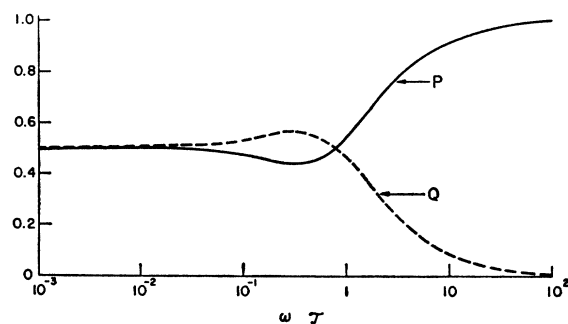


FIG. 2. Variation of P and Q as a function of $\omega\mathcal{T}$ for $A(\phi_A, \phi_B) = C$.

between different sheets of the Fermi surface, large departures from the usual behavior of the transverse magnetoresistance can occur. Restricting our discussion to the case of closed orbits, we note that for noncompensated metals the magnetoresistance can increase (roughly linearly) with the magnetic field strength due to intersheet scattering, and for compensated materials we can expect departures from the quadratic behavior predicted by the Lifshitz-Azbel-Kaganov¹⁸ theory. The Hall resistivity is especially sensitive to the effects of intersheet scattering. For the noncompensated situation, the scattering process can change the number of carriers and thus directly vary the slope of the Hall resistivity as a function of the magnetic field. In the case of metals which are compensated (in the absence of intersheet scattering) various possibilities exist for the behavior of the Hall resistivity ρ_{21} . In particular, as the magnetic field strength is increased, the slope and sign of ρ_{21} can change as the orbits become more nearly compensated. Thus the Hall resistivity can exhibit a transition from electronlike behavior to holelike behavior, or vice versa, due to the influence of the intersheet scattering process.

Recent experimental results for the galvanomagnetic properties of cadmium^{11-13,21} and Cd-Zn alloys^{12,21} display several anomalous features which are quite sensitive to the field strength, impurity concentration, and variations of temperature. The results of Grenier *et al.*¹³ for the Hall resistivity as a function of the magnetic field for a cadmium single crystal of high purity are shown in Fig. 3. Disregarding the high-

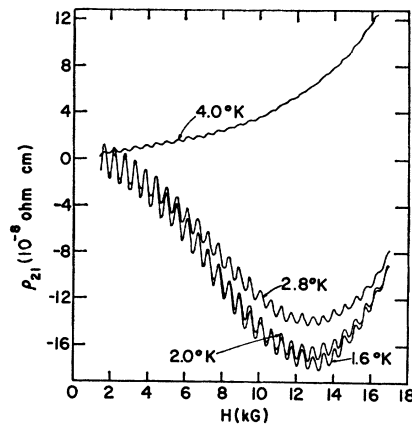
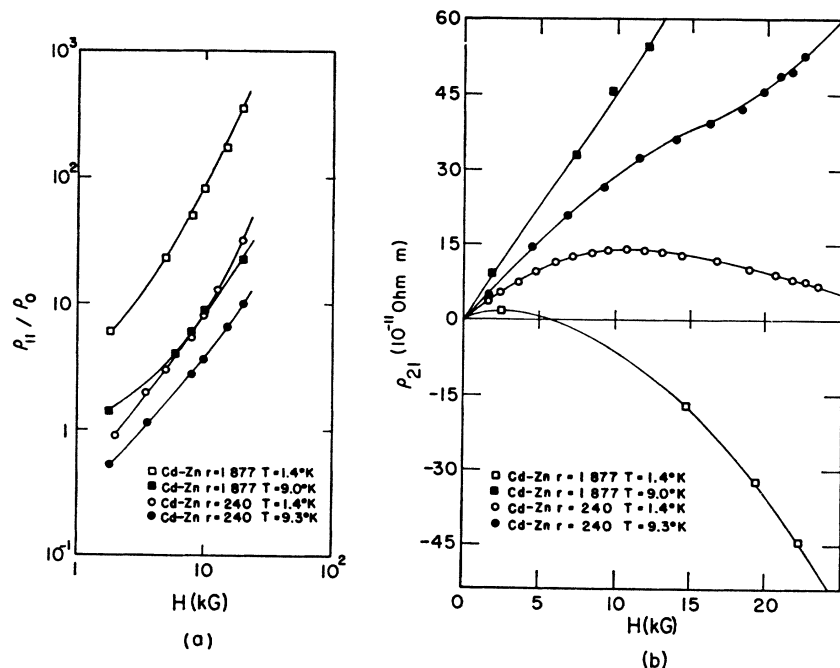


FIG. 3. Experimental results (Ref. 13) for Hall resistivity ($H \parallel [0001]$) of a cadmium sample of high purity; $r = \rho_{300}/\rho_{4.2} \cong 35\,000$. The oscillations are due to magnetomorphic effects.

frequency oscillations of ρ_{21} which are due to magnetomorphic effects, the Hall resistivity exhibits electronlike behavior for very low temperatures ($T \cong 2^\circ\text{K}$), but displays a hole-dominated character for slightly larger temperatures ($T = 4^\circ\text{K}$). A particularly interesting feature of the results shown in Fig. 3 is the slope of ρ_{21} for large magnetic fields, i.e., the Hall resistivity tends to approach holelike behavior in this limit. In addition, the transition from electronlike to holelike behavior of the Hall resistivity as a function of temperature has been investigated for a number of Cd-Zn alloys^{12,21}. Figure 4 displays the results of Refs. 12 and 21 for the

FIG. 4. Experimental results (Refs. 12 and 21) for the transverse magnetoresistance and Hall resistivity of two Cd-Zn alloys as a function of magnetic field ($H \parallel [0001]$). Impurity concentrations are indicated by the residual resistance ratio r .



²¹ O. P. Katyal, A. N. Gerritsen, J. Ruvalds, Richard A. Young, and L. M. Falicov, Phys. Rev. Letters 21, 694 (1968).

Hall resistivity of two *Cd-Zn* alloys. Note that the resistivity changes sign as a function of temperature in a manner similar to the case of pure cadmium, but for low temperatures, $T=1-4^\circ\text{K}$, ρ_{21} is positive for low magnetic fields and then becomes negative, i.e., electronlike for higher fields. For the more impure sample, the influence of impurity scattering is quite large and, as a result, the value of $\omega\tau$, where τ is the relaxation time, is rather small ($\omega\tau \approx 3$ for $H \approx 20$ kG). The effects associated with small $\omega\tau$ values have a marked influence on the magnetoresistance of cadmium and *Cd-Zn* alloys and are discussed in Sec. II.

The purpose of the present work is to investigate the influence of scattering between different sheets of Fermi surface on the galvanomagnetic properties of metals by means of an idealized model for the Fermi-surface topology. In calculating the galvanomagnetic tensors we follow closely the formulation of Falicov and Sievert²² with suitable modifications due to the nature of the scattering mechanism. Section II contains a description of the theoretical calculation. In Sec. III we present the results of the calculation together with a discussion of the applicability of our model to polyvalent metals, with particular emphasis being placed on cadmium.

II. METHOD OF CALCULATION

We begin with a discussion of the physical approximations used to compute the conductivity and resistivity tensors (σ_{ij} and ρ_{ij}) in the presence of a magnetic field for the model Fermi surface shown in Fig. 5(a). Assuming for the moment that impurity scattering (which can be approximated by a screened Coulomb potential) is the dominant mechanism by which electrons (or holes) are scattered into the equilibrium Fermi sea, the scattering probability will be peaked in the forward direction, i.e., the final velocity v_f is likely to be parallel to the initial velocity v_i . For regions such as *A*, *B*, *C*, or *D* in Fig. 5(a), we assume that the total effect of impurity scattering can be described by a relaxation time τ . However, for holes with wave vector \mathbf{k} in the vicinity of points 1, 1', 2, and 2' the relaxation-

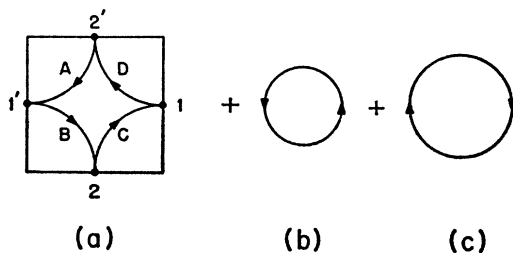


FIG. 5. Sheets of Fermi surface used in the theoretical calculation of the resistivity tensor. Orbits (a) and (b) are holelike in character.

²² L. M. Falicov and P. R. Sievert, *Phys. Rev.* **138**, A88 (1965).

time approximation can no longer be used, since for wave vectors near these points, small-angle scattering ($v_f \approx v_i$) can cause an electron to follow trajectories of the form $A1'1D$ and consequently alter the character of the orbit; e.g., a hole-like orbit $ABCD$ can become totally or at least partly, electronlike ($ADCB$) in character. This type of scattering is equivalent to scattering between different sheets of the Fermi surface in the repeated-zone scheme and will hereafter be called intersheet scattering.

If, for the sake of simplicity, we assume that the intersheet scattering can be localized in a very small region in k space, an electron arriving at one of these "hot spots," say, 1' via branch *A* of the orbit, will have a probability P [eq. (1.1)] of leaving 1' via *B* and a probability $Q=1-P$ of being scattered into 1, continuing thus its trajectory along the branch *D*. In making this "point-scattering" approximation we have essentially compressed the width of the channel Δ (Fig. 1) and increased the strength of the scattering C so that $T^{-1}=C\Delta^2$ remains finite. Thus, in this approximation, the physical significance of C and Δ is lost and T (the typical scattering time) is the only meaningful parameter.

One metal, for example, whose Fermi-surface topology admits the possibility of such intersheet scattering is cadmium. Figure 6 exhibits a schematic illustration of a section in the basal plane of the second band hole sheet of the Fermi surface of cadmium. Regions where intersheet scattering is likely to occur, i.e., the "cloverleaf" tips, are indicated by dots. The above type of scattering can cause a hole to follow an electronlike trajectory such as $ABCDE$, etc., in Fig. 6.

On the basis of the above approximations and using the model Fermi surface shown in Fig. 5(a), we can determine the conductivity tensor by straightforward application of the method of Falicov and Sievert²² which involves the following assumptions:

(a) In the absence of intersheet scattering the electron distribution function f satisfies the Boltzmann equation, with the scattering term given by a relaxation-

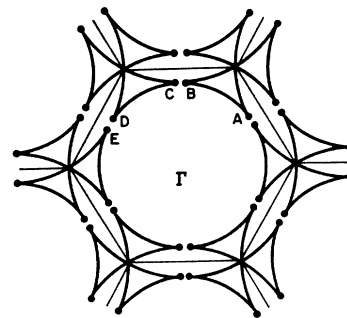


FIG. 6. Schematic cross section in the basal plane of the second band hole sheet of Fermi surface of cadmium. The dots indicate regions where intersheet scattering is likely to occur.

time approximation;

$$\frac{\partial f}{\partial t} + \mathbf{F} \cdot \frac{\partial f}{\partial \mathbf{k}} = -\frac{f - f_0}{\tau}, \quad (2.1)$$

where \mathbf{F} is the external force, f_0 is the equilibrium Fermi-Dirac distribution function, and τ is the relaxation time (assumed to be constant on surfaces of constant energy; thus we neglect the contribution to τ from the intersheet scattering in the hot-spot regions).

(b) The force acting on the electron is the usual Lorentz force, i.e.,

$$\mathbf{F} = \hbar \mathbf{k} = -|e|[\mathbf{E} + (1/c)\mathbf{v} \times \mathbf{H}]. \quad (2.2)$$

If, in the solution of (2.1), terms in the magnetic field \mathbf{H} are included to all orders, but only terms linear in the electric field \mathbf{E} are kept, then, on the basis of the above assumptions, the Boltzmann equation (2.1) may be solved using Chambers's path-integral method and yields the well-known result²²

$$\sigma_{ij} = \frac{-e^2}{4\pi^3} \int_{\text{all } \mathbf{k}} v_i(\mathbf{k}) \frac{\partial f_0}{\partial \epsilon} d^3k \int_{-\infty}^{t(\mathbf{k})} v_j(s) \exp\left(\frac{s-t}{\tau}\right) ds, \quad (2.3)$$

where the time-dependent velocity $v_j(t)$ may be obtained from the set of equations

$$\hbar \dot{\mathbf{k}} = -(|e|/c)\mathbf{v} \times \mathbf{H}, \quad (2.4)$$

$$\mathbf{v}(\mathbf{k}) = (1/\hbar)[\partial \epsilon(\mathbf{k})/\partial \mathbf{k}]. \quad (2.5)$$

In the following discussion we assume explicitly that magnetic breakdown does not occur for the present model. The extension of the Falicov-Sievert theory to include intersheet scattering by means of the two-channel model is then straightforward. In the Falicov-Sievert²² formalism we make the replacement

$$p^2 \rightarrow Q, \quad (2.6)$$

where p^2 is the magnetic-breakdown probability and Q denotes the probability that a particle incident in one channel (or orbit) will be scattered to a different sheet of the Fermi surface. In the limit of very large magnetic fields (corresponding to zero interchannel scattering probability) the fundamental orbit [Fig. 5(a)] is holelike in character. As the magnetic field is *decreased*, the probability Q of intersheet scattering increases and there is a partial transition to a closed (electron) orbit (in addition to extended and open orbits). Unlike the case of magnetic breakdown, however, the model cannot exhibit in any limit a purely electronlike behavior.

On the basis of the above assumptions, the conductivity may be computed in a direct fashion in analogy with the treatment in Ref. 22 and, for the Fermi-surface geometry shown in Fig. 5(a), is given by²²

$$\sigma_{ij} = \frac{-e^2 m \omega}{4\pi^3 \hbar^2} \sum_{l=1}^4 \int \frac{\partial f_0}{\partial \epsilon} d\epsilon \int dk_z \int_0^{t_0} v_i(t', l) I_j(t', l) dt', \quad (2.7)$$

²² R. G. Chambers, Proc. Phys. Soc. (London) A65, 458 (1952); Proc. Roy. Soc. (London) A238, 344 (1956).

where $\omega = eH/mc$, $t_0 = \pi/2\omega$,

$$I_j(t', l) = \exp\left(\frac{-t'}{\tau}\right) \left[\int_0^{t'} v_j(s', l) \exp\left(\frac{s'}{\tau}\right) ds' + K_j(l) \right], \quad (2.8)$$

and the column vector $K_j(l)$ can be expressed in the form

$$\mathbf{K}_j = \mathbf{M} \exp(-t_0/\tau) \cdot [\mathbf{I} - \mathbf{M} \exp(-t_0/\tau)]^{-1} \cdot \mathbf{V}_j. \quad (2.9)$$

For the present model, the column vector $V_j(\mathbf{r})$ is defined by

$$V_j(\mathbf{r}) = \int_0^{t_0} v_j(s', \mathbf{r}) \exp\left(\frac{s'}{\tau}\right) ds' \quad (r=1,2,3,4) \quad (2.10)$$

and the matrix \mathbf{M} , which takes into account the effects of intersheet scattering, is given by

$$\mathbf{M} = \begin{pmatrix} 0 & Q & P & 0 \\ 0 & P & Q & 0 \\ P & 0 & 0 & Q \\ Q & 0 & 0 & P \end{pmatrix}, \quad (2.11)$$

where Q is the interchannel scattering probability and $P=1-Q$. Substitution of (2.11) and (2.10) into (2.9), (2.8), and finally (2.7) yields the conductivity tensor σ_{ij} and, by inverting the tensor σ_{ij} , also gives ρ_{ij} .

The magnetoresistance ρ_{11} and the Hall resistivity ρ_{21} were calculated numerically using the above procedure for a number of Fermi-surface geometries. The results and their application to cadmium are discussed in Sec. III.

III. RESULTS AND DISCUSSION

The results for various combinations of the sheets of Fermi surface shown in Fig. 5 are presented as follows: (1) Basic sheet only [Fig. 5(a)]; results are shown in Fig. 7. (2) Basic sheet plus one noncompensating electron sheet, $n_e/n_a=0.5$, Figs. 5(a) and 5(c); results

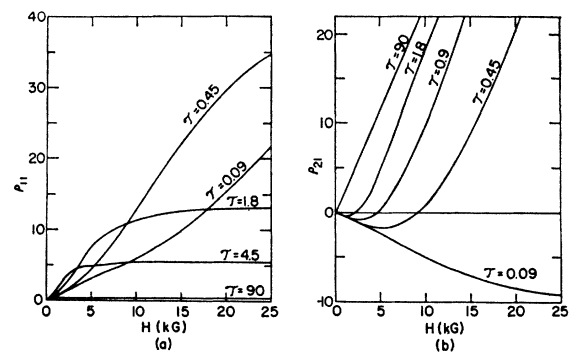


FIG. 7. Calculated transverse magnetoresistance (a) and Hall resistivity (b) for the single holelike sheet of Fermi surface shown in Fig. 5(a) (case 1). Intersheet scattering generates closed electronlike orbits. The parameter \mathcal{T} is measured in units of 10^{-11} sec, $T=1^\circ\text{K}$, and $\tau=9.2 \times 10^{-10}$ sec.

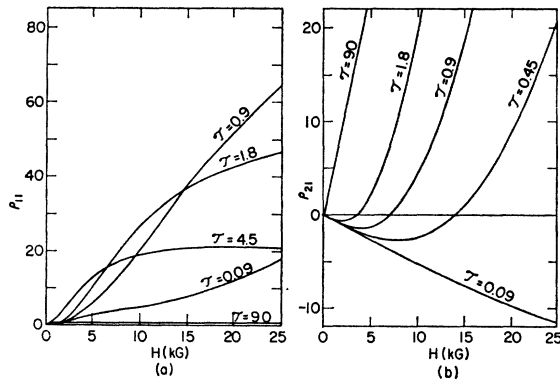


FIG. 8. Calculated transverse magnetoresistance (a) and Hall resistivity (b) for case 2, i.e., partially compensated orbits; Figs. 5(a) and 5(c). The parameter \mathcal{T} is measured in units of 10^{-11} sec, $T=1^\circ\text{K}$, and $\tau=9.2 \times 10^{-10}$ sec.

are given in Fig. 8. (3) Basic sheet plus one compensating electron orbit, Figs. 5(a) and 5(c); results are given in Fig. 9. (4) Basic sheet plus an additional hole sheet and a compensating electron sheet, $n_a+n_b=n_c$, $n_a/n_b=0.5$, Figs. 5(a)–5(c); results are shown in Figs. 10 and 11.

In the calculation of the conductivity tensor the relaxation time τ for all sheets of the Fermi surface was taken to be

$$1/\tau = A + BT^5, \quad (3.1)$$

where A and B were obtained from the experimental data for cadmium.^{11,12} The cyclotron masses for the various Fermi-surface pieces shown in Fig. 5 are as follows: $m_a^*=0.4$, $m_b^*=0.2$, and $m_c^*=0.7$, with corresponding cyclotron frequencies $\omega_i = |e|H/m_i^*c$, $i=a,b,c$.

The results for cases 1 and 2 [Figs. 7(a) and 8(a)] show a qualitative similarity to the experimental results for the transverse magnetoresistance of aluminum.¹⁷ Although the present model is not intended to describe

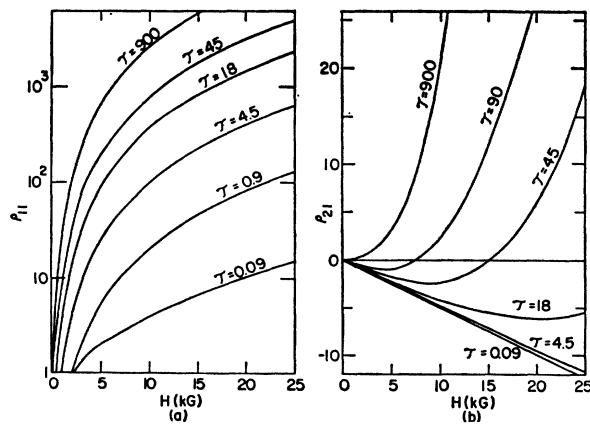


FIG. 9. Calculated transverse magnetoresistance (a) and Hall resistivity (b) for the compensated orbits shown in Figs. 5(a) and 5(c); case 3. The parameter \mathcal{T} is measured in units of 10^{-11} sec, $T=1^\circ\text{K}$, and $\tau=9.2 \times 10^{-10}$ sec.

the Fermi surface of aluminum, the above qualitative agreement indicates that small-angle scattering effects can provide an explanation for the deviation from the expected behavior of the magnetoresistance (see Table I).

For case 3, shown in Fig. 9, it is interesting to note the transition from electronlike to holelike behavior of the Hall resistivity ρ_{21} as the magnetic field is increased. Also, the magnetoresistance ρ_{11} deviates slightly from the expected H^2 dependence, i.e., it behaves as $\rho_{11} \approx \text{const} \times H^{1.9}$ for the present case.

We now turn our attention to case 4, which provides a remarkable description of the galvanomagnetic properties of cadmium and Cd-Zn alloys when the magnetic field is parallel to the [0001] direction. The basic hole sheet Fig. 5(a) is taken to represent the two pieces of the cadmium "monster" in the second zone close to the basal plane¹¹ (see Fig. 6). In addition, a second sheet of hole orbits [Fig. 5(b)] is included to represent the sections of the second-zone monster close to the "necks" as well as the orbits on the first-zone "caps." Finally, the compensating sheet of electronlike orbits represents the electrons in the third-zone "lens" of cadmium. The calculated magnetoresistance and Hall resistivity for case 4 are displayed in Figs. 10 and 11. These curves exhibit a striking similarity to the experimental results shown in Figs. 3 and 4. In obtaining the theoretical results, the parameter \mathcal{T} , which is a typical scattering time for the two-channel model, was adjusted to fit the calculated curves to the experimental results.

The influence of the intersheet scattering is most dramatic for the Hall resistivity ρ_{21} [Figs. 10, 11(b), and 11(c)]. The various results for ρ_{21} corresponding to different values of τ and \mathcal{T} (i.e., to different tempera-

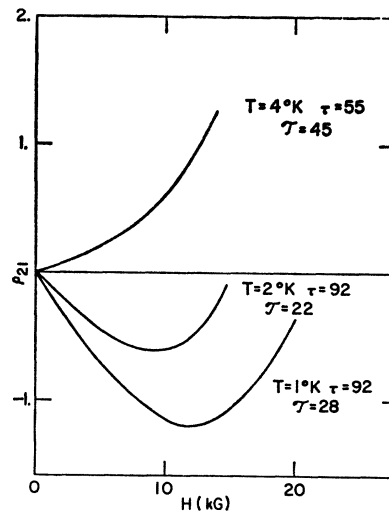
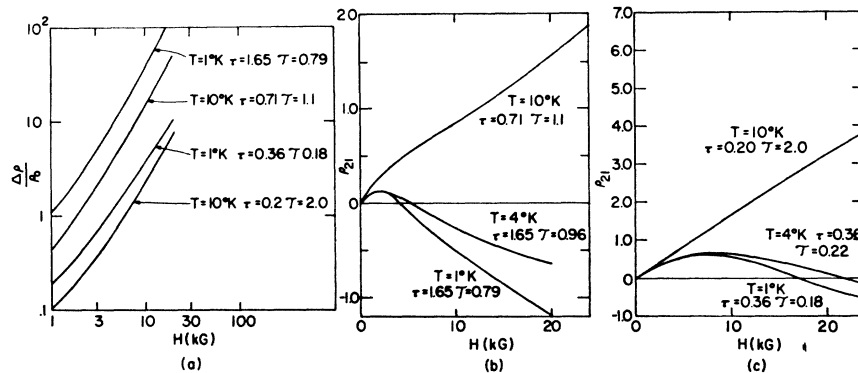


FIG. 10. Calculated Hall resistivity for the orbits shown in Figs. 5(a)–5(c); case 4. The parameters τ and \mathcal{T} were chosen to represent the experimental case shown in Fig. 3, and are measured in units of 10^{-11} sec.

FIG. 11. (a) Calculated transverse magnetoresistance; (b) and (c) Hall resistivity for the orbits shown in Figs. 5(a)-5(c); case 4. The parameters τ and \mathcal{T} were adjusted to fit the experimental results shown in Fig. 4, and are measured in units of 10^{-11} sec.



tures and impurities) can be qualitatively understood as follows.

(1) For magnetic field strengths such that $\omega_b\tau < 1$, the small mass of the holes ($m_b=0.2$) dominates and ρ_{21} is always positive. This effect can be seen in Figs. 11(b) and 11(c).

(2) For magnetic fields such that $\omega_c\tau > 1$ while $\omega_a\mathcal{T} < 1$, all the charge carriers are in the high-field region but the intersheet scattering generates electron-like trajectories (in addition to extended and open orbits). Under these conditions the number of effective electrons is greater than the number of effective holes and ρ_{21} tends to become negative. This behavior can be seen, for example, in the case $T=4^\circ$, $\tau=1.65 \times 10^{-11}$ sec, $\mathcal{T}=9.6 \times 10^{-12}$ sec in Fig. 11(b). The negative trend in ρ_{21} continues into the region where $\omega_c\tau > 1$ and $\omega_a\mathcal{T} \geq 1$ as exhibited by the curve for $T=1^\circ$, $\tau=9.2 \times 10^{-10}$ sec, $\mathcal{T}=2.8 \times 10^{-10}$ sec (Fig. 10).

(3) When $\omega_a\mathcal{T} \gg 1$, the compensation between electrons and holes is restored and the holes dominate once again, causing ρ_{21} to have a positive slope. This very-high-field regime can be seen, for instance, for $T=2^\circ$, $\tau=9.2 \times 10^{-10}$ sec, $\mathcal{T}=2.2 \times 10^{-10}$ sec in Fig. 10.

(4) When τ and \mathcal{T} are of the same order of magnitude or when $\mathcal{T} > \tau$, the negative region of ρ_{21} cannot be reached and ρ_{21} is positive for all values of H as in the case of $T=10^\circ$, $\tau=7.1 \times 10^{-12}$ sec, $\mathcal{T}=1.1 \times 10^{-11}$ sec in Fig. 11(b).

From the values of τ and \mathcal{T} (Figs. 10 and 11) used in the calculations it is apparent that impurity scattering is the principal mechanism which gives rise to intersheet scattering. This can be seen from the increase of \mathcal{T}^{-1} (which is proportional to the strength of the scattering) with increasing impurity concentration. Also, the fact that \mathcal{T}^{-1} decreases with increasing temperature indicates that electron-phonon scattering tends to destroy the coherence necessary for intersheet scattering to be effective. One possible mechanism by which this coherence destruction takes place can be seen by considering the geometry of the cadmium Fermi surface near the regions where intersheet scattering is important. One such region is that labeled by *B*, *C* in

Fig. 6. We can see that for such a region the component of the velocity parallel to a line joining *B* and *C* is randomized during interchannel scattering while the velocity component perpendicular to such a line remains constant. It is the conservation of the latter velocity component which provides the coherence effects that markedly influence the galvanomagnetic properties. If we now admit the possibility of phonon scattering, then near the hot-spot regions a phonon with very small wave vector \mathbf{q} ($|\mathbf{q}| \ll k_F$) can scatter holes in such a way as to randomize the formerly conserved velocity component and thus weaken the coherence properties of the channel. This weakening of the coherence of the interchannel scattering is reflected in a decrease of \mathcal{T}^{-1} as the temperature is increased. The above discussion is meant only as a qualitative description of one possible mechanism by which electron-phonon scattering can destroy the effects of intersheet scattering. The details of such a mechanism or any other mechanism would require a detailed study of the electron-phonon interaction in cadmium.

It is worthwhile to remark that the location of the minimum of ρ_{21} at low temperatures ($T \approx 1^\circ\text{K}$) depends only on the value of $\omega_a\mathcal{T}$ and consequently is quite sensitive to the concentration of impurities. This suggests that experimental measurements of the location of the above minimum as a function of impurity concentration would provide a quantitative determination of the influence of impurity scattering on \mathcal{T} .

In conclusion, the model Fermi surface considered above appears to account for the observed galvanomagnetic properties (with $\mathbf{H} \parallel [0001]$) of cadmium and some *Cd-Zn* alloys and thus gives a dramatic illustration of the inadequacy of using *only* a relaxation-time approximation in dealing with transport properties of polyvalent metals.

ACKNOWLEDGMENTS

We would like to acknowledge several stimulating discussions and exchange of information with O. P. Katyal, Professor A. N. Gerritsen, and Professor R. W. Stark.